Fabrication of Self-Ordered Porous Alumina via Etidronic Acid Anodizing and Structural Color Generation from Submicrometer-Scale Dimple Array

Tatsuya Kikuchi*[,1], Osamu Nishinaga, Shungo Natsui, and Ryosuke O. Suzuki
Faculty of Engineering, Hokkaido University
N13-W8, Kita-ku, Sapporo, Hokkaido, 060-8628, Japan

* Corresponding author: Tatsuya Kikuchi
TEL: +81-11-706-6340
FAX: +81-11-706-6342
E-mail: kiku@eng.hokudai.ac.jp

[1] ISE active member

Abstract

Highly ordered anodic porous alumina with a large-scale cell diameter was successfully fabricated via anodizing in a new electrolyte, etidronic acid (1-hydroxyethane-1,1-diphosphonic acid). High-purity aluminum specimens were anodized in a 0.3 M etidronic acid solution under constant current density and voltage conditions. Etidronic acid anodizing at 210 to 270 V at the appropriate temperature caused the anodic porous alumina to exhibit self-ordering behavior, and periodic nanostructures measuring 530 to 670 nm in cell diameter were fabricated on the aluminum substrate. The self-ordering voltage and the corresponding cell diameter could be increased without burning by systematically increasing the stepwise voltage. Two-step etidronic acid anodizing without nanoimprinting can easily yield the formation of highly ordered anodic porous alumina with a large-scale cell diameter. A submicrometer-scale dimple array fabricated via etidronic acid anodizing and subsequent selective oxide dissolution gave rise to bright structural color with a rainbow distribution.

Keywords: Anodizing; Etidronic Acid; Anodic Porous Alumina; Self-Ordering; Structural Color

1. Introduction

Anodizing aluminum and its alloys in acidic electrolyte solutions results in the formation of porous anodic oxide films (anodic porous alumina) with numerous nanometer-scale pores [1-3]. Most importantly, anodic porous alumina is self-ordered when anodized under the appropriate electrochemical conditions in a given acidic solution, and consequently, high-aspect-ratio anodic porous alumina with an ideal cell arrangement can be easily obtained [4-9]. In the self-ordering anodizing, it is well known that the cell diameter of the anodic porous alumina, D, is strongly related to the self-ordering voltage, U_s: a) D = 50-60 nm at U_s = 19-25 V for sulfuric acid [10,11], b) 100 nm at 40 V for oxalic acid [4,11,12], c) 95-112 nm at 42-48 V for selenic acid [13,14], d) 300 nm at 120 V for malonic acid [15], e) 405-500 nm at 160-195 V for phosphoric acid [16,17], and f) 500 nm at 195 V for tartaric acid [15]. Ordered anodic porous alumina is most commonly obtained by anodizing at voltage values close to these ordering voltages. In addition, advanced anodizing procedures involving effective experimental approaches, including hard anodizing [18-21] and the use of an electrolyte mixture [22-24], have been reported by several research groups to increase the self-ordering voltage and the corresponding cell diameter of self-ordered anodic porous alumina. Such anodic porous alumina is widely used in various nanoscience and engineering applications, including plasmonic devices [25,26], anti-reflection sheets [27,28], photonic crystals [29,30], diodes [31], nanocontainers [32], nanofilters [33,34], gas sensors [35-36], and magnetic nanomaterials [37].

Because the cell diameter of self-ordered porous alumina fabricated by typical anodizing in aqueous solutions is limited to approximately 500 nm at 200 V [5,18], larger cell diameters that correspond to visible-light wavelengths ranging between 500 nm and 800 nm are required to expand the applicability of porous alumina in the field of optics. Malic acid anodizing provides a relatively high anodizing voltage and, consequently, a larger cell diameter, D = 300-800 nm at 200-350 V [38,39]. However, to date, ordered anodic porous alumina has not been obtained by malic acid anodizing. As an alternative electrolyte for high-voltage anodizing, citric acid has also been investigated by several research groups [39-42]. Citric acid anodizing operates over an anodizing voltage range of approximately 260-540 V. However, non-uniform black oxides are easily formed by a phenomenon called “burning” during citric acid anodizing because of localized breakdown under high electric fields, and it is difficult to obtain high-aspect-ratio ordered porous alumina. Therefore, ethylene glycol mixture solutions containing citric acid and other electrolytes have been developed for steady-state oxide growth to avoid burning during anodizing [43,44]. Anodic porous alumina, which possesses a large-scale cell size greater than 500 nm, can be successfully formed by anodizing in these mixture solutions. However, the following problems continue to affect the fabrication of ordered anodic porous alumina: a) complicated electrolyte formulations containing organic solvents and several electrolytes and b) the need to perform nanoimprinting before anodizing, as previously reported. Therefore, a novel

high-voltage anodizing technique involving a simple electrolyte solution for self-ordering must be developed to fabricate ordered anodic porous alumina with larger cell diameters. Very recently, several research groups have reported the novel electrolytes for anodic porous alumina, although large-scale porous alumina could not be obtained [45-49].

Herein, we demonstrate the fabrication of self-ordered anodic porous alumina via etidronic acid (1-hydroxyethane-1,1-diphosphonic acid, $CH_3C(OH)[PO(OH)_2]_2$, H_4ET) anodizing. Etidronic acid is currently one of the most popular chelating agents and is widely used in various applications, such as in medicines, commercial washing agents, and inhibitors for corrosion protection. Etidronic acid is a tetraacid that features four acidic hydroxyl groups with the following acid dissociation constants, pKa [50,51]:

$$H_4ET \rightleftarrows H^+ + H_3ET^- \qquad (pKa_1 = 1.43) \qquad (1)$$

$$H_3ET^- \rightleftarrows H^+ + H_2ET^{2-} \qquad (pKa_2 = 2.70) \qquad (2)$$

$$H_2ET^{2-} \rightleftarrows H^+ + HET^{3-} \qquad (pKa_3 = 7.02) \qquad (3)$$

$$HET^{3-} \rightleftarrows H^+ + ET^{4-} \qquad (pKa_4 = 11.20) \qquad (4)$$

Because etidronic acid possesses low pKa values, particularly low pKa_1 and pKa_2 values as indicated above, it is expected that etidronic acid has the potential to behave as a suitable electrolyte for fabricating anodic porous alumina. We found that etidronic acid anodizing under appropriate electrochemical conditions provided highly ordered anodic porous alumina with a large-scale cell diameter, approximately 530-670 nm. It should be noted that the cell diameter corresponds to a wide region of the visible-light spectrum. Therefore, nanostructures fabricated by etidronic acid anodizing exhibit unique optical properties, such as structural coloration with a rainbow color distribution. This paper describes in detail the electrochemical behavior of self-ordered anodic porous alumina during etidronic acid anodizing and the nanomorphology of the material. Simultaneously, we report a novel structural color aluminum reflector fabricated by etidronic acid anodizing and its optical properties.

2. Experimental

2.1 Etidronic acid anodizing

High-purity aluminum specimens (99.999 wt%, 0.25-1.0 mm thick, GoodFellow, UK) were ultrasonically degreased in an ethanol solution for 10 min. After degreasing, the lower half of the handle of the specimens was coated with silicone resin, and the specimens were electropolished in a 13.6 M CH_3COOH/2.56 M $HClO_4$ mixture at 28 V for 1 min. The electropolished specimens were then immersed in a 0.3 M etidronic acid solution (Sigma-Aldrich, USA, T = 273-333 K) and were anodized at a constant current density of j = 10-30 Am^{-2} and a constant cell voltage of U = 145-295 V for up to 72 h. During the initial stage of constant voltage anodizing, the voltage was increased linearly for 2.5 min and then held constant using a PC-connected direct current power supply (PWR-400H, Kikusui, Japan). For ultra-high voltage anodizing, the voltage was increased stepwise at 120-min intervals during anodizing (stepwise voltage increase

anodizing). A platinum plate (99.95 wt%, 0.10 mm thick, Nilaco, Japan) was used as the counter electrode, and the electrolyte solution was vigorously stirred with a magnetic stirrer during anodizing.

After anodizing, the specimens were immersed in a 0.20 M CrO_3/0.51 M H_3PO_4 solution (T = 353 K) to selectively dissolve the anodic oxide. The aluminum, whose nanostructure corresponded to the shape of the bottom of the anodic oxide, was exposed to the surface. The exposed specimens were then anodized once again in a 0.3 M etidronic acid solution (293 K) at a constant voltage of V = 270 V to obtain a highly ordered anodic porous alumina from the top surface to the bottom interface (two-step anodizing). After each chemical step, the specimens were immediately removed from the solutions and then washed with distilled water and dried in a desiccator.

2.2 Characterization of the anodic porous alumina

The surface and fractural cross-section of the anodized and aluminum-exposed specimens were examined by field-emission scanning electron microscopy (FE-SEM, JSM-6500F and JIB-4600F/HKD, JEOL, Japan). A thin platinum electro-conductive layer was coated on the specimens by a sputter coater (MSP-1S, Vacuum Device, Japan) to observe the anodic oxide. Optical reflectance measurements of the nanostructured aluminum surface were also performed. The aluminum specimens were irradiated with a white light source (HL-2000, Ocean Optics, USA) through an optical fiber, and the reflected light was measured by a multi-channel spectrometer (USB2000+, Ocean Optics, USA). During the optical measurements, each aluminum specimen was rotated by a θ-axis stage from 25.0 to 45.0°.

3. Results and Discussion

3.1 Constant current density anodizing and anodic porous alumina formation

Figure 1a shows the changes in the anodizing voltage, U, with time, t, in a 0.3 M etidronic acid solution at 293 K at different constant current densities of j = 10-30 Am^{-2} over a period of 60 min. At each current density, the voltage initially increased linearly, reached a peak value, decreased slightly, and finally reached a steady value. This characteristic electrochemical behavior is highly similar to that measured by anodizing in acidic electrolytes such as sulfuric, oxalic, selenic, and phosphoric acid solutions for anodic porous alumina fabrication. Therefore, the voltage-time transients strongly suggest that etidronic acid anodizing caused the formation of anodic porous alumina on the aluminum specimens. The anodizing voltage in the plateau region increased with the applied current density, reaching values of approximately 160-220 V. It should be noted that the voltages above 200 V were higher than the voltages measured for phosphoric acid anodizing because a higher anodizing voltage causes a larger cell diameter to form in anodic porous alumina.

Figure 1b shows an SEM image of the surface of the specimen anodized in etidronic acid solution at 30 Am^{-2} for 60 min. Numerous nanopores with a

non-periodical arrangement can be observed over the entire surface of the specimen. The anodic oxide was selectively removed from the aluminum substrate by chemical dissolution, and an SEM image of the exposed aluminum surface (specifically, the interface between the anodic oxide and aluminum substrate) is shown in Fig. 1c. Disordered submicrometer-scale dimples measuring approximately 500 nm in diameter were distributed over the aluminum substrate. Figure 1d shows an SEM image of the vertical cross-section of the specimen; the gray region at the top corresponds to an epoxy resin, and the rough surface region at the bottom corresponds to the aluminum substrate. An anodic oxide film measuring 7 μm in thickness with vertical nanopores was uniformly formed on the aluminum substrate. As indicated by the SEM images shown in Figs. 1b through 1d, etidronic acid anodizing clearly created an anodic porous alumina, although the cell arrangement was disordered under the constant-current anodizing condition. For the fabrication of self-ordered anodic porous alumina, constant-voltage anodizing is generally performed. Therefore, the details of the electrochemical behavior and the corresponding nanofeatures of the alumina under constant-voltage anodizing in an etidronic acid solution were examined to identify the self-ordering behavior of the anodic porous alumina.

3.2 Constant-voltage anodizing under various conditions

Figure 2a shows the changes in the current density, j, with anodizing time, t, at constant anodizing voltages of V = 250-275 V in a 0.3 M etidronic acid solution (293 K). During anodizing, the voltage increased linearly during the initial 2.5 min and then was held constant at a predetermined value. After the initial increase in voltage, the current densities decreased rapidly to approximately 10 Am^{-2} from 50 Am^{-2} at each voltage and then increased rapidly. This electrochemical behavior is typically observed during constant-voltage anodizing in acidic electrolyte solutions due to barrier oxide formation and the subsequent initiation of nanopore formation in the oxide. The current densities then reached steady values upon further anodizing at 250, 260, and 270 V due to the steady-state growth of the anodic oxide. In contrast, the current density rapidly increased to values above 150 Am^{-2} at 275 V after the initial stage, and oxygen gas was generated from the aluminum specimen. This “burning” phenomenon is observed due to the high current density in localized regions caused by the high electric field applied, which results in non-uniform oxide formation. The current density during steady-state growth increased with the anodizing voltage due to the high growth rate of the anodic oxide under high-voltage anodizing. It should be noted that the anodizing voltages for steady growth during etidronic acid anodizing are considerably higher than those used in typical acidic electrolytes, such as sulfuric, oxalic, selenic, and phosphoric acid.

Figure 2b shows the current-time transients during etidronic acid anodizing (273 K) at several constant anodizing voltages of U = 270-295 V. Comparing Fig. 2b with Fig. 2a, the highest anodizing voltage for steady growth at 273 K (290 V) was higher than that at 293 K (270 V). However, the current density at the highest voltage

decreased to below 10 Am^{-2}, j = 6 Am^{-2}. In addition, the growth rate of the anodic oxide also decreased with the solution temperature, although higher anodizing voltages could be applied to the specimen. Furthermore, the current densities at 280 V and 290 V exhibited an unstable oscillation. It is expected that such a slow growth rate and the unstable electrochemical behavior observed at low temperature are unsuitable for the formation of self-ordered anodic porous alumina.

Figure 3 shows the current-time transients during etidronic acid anodizing at high solution temperatures of a) T = 298, b) 303, c) 313, and d) 333 K under constant-voltage conditions. In contrast to the voltages observed during low-temperature anodizing, the highest anodizing voltage for steady growth without burning decreased with increasing temperature: 240 V at 298 K, 225 V at 303 K, 210 V at 313 K, and 165 V at 333 K. The effects of the temperature on the highest anodizing voltage during etidronic acid anodizing were summarized in Fig. 4. However, the current density increased with solution temperature: 125 Am^{-2} at 298 K, 150 Am^{-2} at 303 K, 190 Am^{-2} at 313 K, and 260 Am^{-2} at 333 K. Therefore, etidronic acid anodizing at high temperature is suitable for the rapid fabrication process of anodic porous alumina.

To summarize the findings obtained regarding the electrochemical behavior of the specimens under constant-voltage anodizing, the highest anodizing voltage for the steady-state growth of anodic porous alumina without burning decreased as the solution temperature increased. The current density at the highest voltage increased with solution temperature. The regularity of the anodic porous alumina formed under these electrochemical conditions, especially while anodizing at the highest voltage without burning, is discussed in detailed below.

3.3 Fabrication of highly ordered anodic porous alumina with a large cell diameter

Figure 5 shows SEM images of the exposed aluminum substrate after etidronic acid anodizing at 313 K and a) 190 V, b) 200 V, and c) 210 V for 120 min. At 190 V, disordered a submicrometer-scale dimple array was distributed over the aluminum substrate, and a large number of dimple junctions with four or five points were observed because of the incomplete self-ordering of the anodic porous alumina. However, the regularity of the anodic porous alumina was clearly improved as the anodizing voltage increased (Figs. 5b and 5c), and a highly ordered submicrometer-scale dimple array with an ideal cell arrangement could be fabricated via etidronic acid anodizing at 210 V. Thus, etidronic acid could serve as a new self-ordering electrolyte for anodic porous alumina fabrication. This self-ordering behavior is easily achieved under high-voltage anodizing without burning, and it is unnecessary to use a complex mixture electrolytes or the powerful cooling stage employed to perform “hard anodizing”. The cell diameter of the highly ordered dimple array fabricated at 210 V was measured to be 530 nm; such a large diameter cannot be achieved by conventional phosphoric acid anodizing.

Etidronic acid anodizing at voltages above 215 V at 313 K as limited by the burning phenomenon, as shown in Fig. 3c. However, the fabrication of highly ordered

anodic porous alumina with a larger cell diameter could be realized by adjusting the optimum solution temperature and electrochemical conditions. Figure 6 shows SEM images of an ideal cell arrangement fabricated by etidronic acid anodizing a) at 225 V and 303 K for 480 min, b) at 240 V and 298 K for 480 min (8 h), and c) at 270 V and 293 K for 960 min (16 h). In this case, it should be noted that each applied anodizing voltage produced the highest electric field that could be achieved without burning at each solution temperature (Figs. 2 and 3). Ideal hexagonal dimples measuring a) 560 nm, b) 600 nm, and c) 670 nm in diameter were formed on the aluminum substrate, and the cell diameter increased with anodizing voltage. Accordingly, etidronic acid anodizing achieved self-ordering with a wide range of diameters larger than 500 nm. On the other hand, disordered dimple arrays were obtained by etidronic acid anodizing at 333 K at voltages ranging from 145 to 165 V. The self-ordering voltage during sulfuric, oxalic, selenic, and phosphoric acid anodizing was limited to each specified range, and etidronic acid anodizing was also limited to approximately 200 V for self-ordering to occur.

High-voltage anodizing at voltages such as 270 V could be carried out not only at 293 K but also at a solution temperature as low as 273 K (Fig. 2), although the current density was relatively small value during anodizing. However, ordered anodic porous alumina could not be obtained under such low-current-density conditions. Fig. 7 shows SEM images of the exposed dimple arrays fabricated by etidronic acid anodizing a) at 270 V and 293 K for 120 min and b) at 270 V and 273 K for 4320 min (72 h). The thicknesses of the anodic porous alumina specimens obtained under these electrochemical conditions were determined by obtaining cross-sectional observations of the anodized specimens and were measured to be 42 μm and 77 μm, respectively. An ordered dimple array was observed on the specimen anodized at 293 K, although a slight defect still remained in the arrangement due to the short anodizing duration. However, a disordered dimple array with different cell diameters was clearly observed on the specimen anodized at 273 K, although the same anodizing voltage was applied to the specimens. Thus, low-current density anodizing caused the formation of disordered anodic porous alumina even if the appropriate self-ordering voltage was applied to the specimen. To fabricate highly ordered anodic porous alumina, anodizing must be carried out under the highest voltage condition that can be achieved without burning at each solution temperature.

Based on the SEM observations shown in Figs. 5 and 6, self-ordering of anodic porous alumina occurs over a wide range of voltages, approximately 210-270 V, during etidronic acid anodizing. However, anodizing by increasing the voltage in a stepwise manner is useful for the fabrication of ordered porous alumina with a larger cell diameter. Figure 8a shows the changes in current density with anodizing time during etidronic acid anodizing (293 K) by a) applying a voltage directly and b) increasing the voltage in a stepwise manner; the first anodizing was performed at 270 V for 120 min, the second anodizing at 275 V for 120 min, and the third anodizing at 280 V for 120

min. When a voltage of 275 V was directly applied to the specimen after the initial increase, the current density rapidly increased to above 200 Am^{-2} due to the burning phenomenon, and non-uniform anodic oxide was formed on the aluminum specimen. Conversely, anodizing by increasing the voltage in a stepwise manner yielded a relatively steady current density without burning at each anodizing voltage, although the plateau current density gradually increased with the applied voltage. Figure 8b shows an SEM image of the exposed aluminum surface anodized using a stepwise voltage increase. A well-ordered, submicrometer-scale dimple array with a cell diameter of approximately 710 nm could be successfully fabricated. Based on these experimental results, anodizing by increasing the voltage in a stepwise manner increases the self-ordering voltage for producing highly ordered anodic porous alumina.

Figure 9 shows SEM images of the fracture cross-section of the anodic porous alumina fabricated by two-step etidronic acid anodizing. To produce this alumina specimen, the anodizing was carried out via the following three procedures; a) anodizing in an etidronic acid solution at 293 K and 270 V for 16 h, b) selective dissolution of the anodic porous alumina in a CrO_3/H_3PO_4 solution at 353 K, and c) a second anodizing step carried out under the same conditions for 120 min. An ordered anodic porous alumina specimen with cell diameters of approximately 670 nm and pore diameters of approximately 250 nm could be successfully fabricated by two-step anodizing in etidronic acid. The porous oxide possessed parallel cylindrical nanoholes without an intercrossing structure. Two-step anodizing caused the formation of highly ordered anodic porous alumina through the top surface to the bottom interface without nanoimprinting and could also be applied at the other self-ordering voltages indicated in Figs. 5 and 6.

Figure 10a summarizes the change in the self-ordering voltage, U_s, with solution temperature, T, during etidronic acid anodizing. The self-ordering voltage decreased with the increase in temperature because of the active dissolution of the anodic oxide into the solution at the bottom of the pores during high-temperature anodizing. Using this relationship, we can predict the self-ordering voltage and the corresponding appropriate electrolyte temperature for the fabrication of highly ordered anodic porous alumina. Moreover, anodizing via a stepwise voltage increase, as shown in Fig. 8, caused a slight increase in the self-ordering voltage without burning, which resulted in an increase in the cell diameter. Although anodizing via a stepwise voltage increase is not appropriate for the fabrication of ordered anodic porous alumina through the top surface to the bottom interface because the cell diameter changes during anodizing, this technique allowed for the fabrication of a highly ordered dimple array with a large cell diameter on the aluminum substrate. Figure 10b summarizes the self-ordering voltages, U_s (V), and the corresponding cell diameters, D (nm), obtained under ordering conditions in etidronic acid and previously reported values for anodizing in aqueous electrolytes, including sulfuric, oxalic, selenic, malonic, phosphoric, and tartaric acid solutions. The linear relationship between the ordering voltage and the cell diameter

during anodizing in aqueous solutions is described as follows:

$$D = 2.5\ U_s\ (nm) \qquad (5)$$

where 2.5 (nmV^{-1}) corresponds to the proportionality constant in the figure. The relation obtained in etidronic acid solution is consistent with those previously reported for other anodizing electrolytes. It should be noted that our electrolyte greatly expands the self-ordering region, 530-670 nm at 210-270 V, which corresponds to a wide range of the visible-light spectrum. Therefore, the fabricated nanostructures exhibited a unique optical property, as described in the next section. Highly ordered anodic porous alumina with a large-scale cell diameter and a subsequently fabricated dimple array can be used for various applications in nanotechnology.

3.4 Bright structural color of the nanostructured aluminum substrate

As illustrated in Figs. 5 through 8, a highly ordered submicrometer-scale dimple array could be obtained on an aluminum substrate via etidronic acid anodizing and subsequent selective dissolution of the anodic oxide. In this study, we found that the aluminum surface covered with the periodic dimple structure displayed bright structural coloration with a rainbow spectrum. Figure 11a shows the surface of the aluminum specimen fabricated by etidronic acid anodizing at 270 V for 16 h and oxide dissolution; the photographs were obtained at different viewing angles. The nanostructured surface clearly shows violet, blue, light blue, green, yellow, orange, and red hues. Although a slightly different coloration appears at the top and edges of the specimen due to the distortion produced by cutting, almost the entire specimen surface is covered by an individual color at each angle. It should be noted that these colors are only generated from the periodic dimple structures of aluminum, not anodic porous alumina combined with metal deposits or organic dyes used in typical coloring techniques.

Changes in the reflection of the dimple array formed on the aluminum substrate, R, with wavelength, λ, are demonstrated in Fig. 11b. During optical measurement, the specimen was rotated to 25.0° from 45.0° by a θ-axis stage, as described in Fig. 11c. The reflection spectrum shows a broad peak at wavelengths of approximately 490-575 nm at the lowest angle of 25.0°. The position of the reflection peak shifts gradually with the rotation angle toward longer wavelengths, reaching 760 nm at 45.0°. As indicated by these optical measurements, the color reflected from the dimple array could easily be controlled to range from blue to red via the fine rotation of the specimen. Such nanostructured aluminum specimens may be used as the imprint mold of an ordered dimple array for the nanoimprinting of other metals and polymers. The structural color reflection over the visible-light spectrum obtained from the large-scale periodic dimple array can be employed in various optical applications, such as in photonic crystals, color displays, sensors, and diffraction gratings.

4. Conclusions

We demonstrated a novel self-ordering electrolyte, etidronic acid, for the

formation of anodic porous alumina with a large-scale cell diameter. Highly ordered anodic porous alumina with a cell diameter measuring 530-670 nm could be successfully fabricated via etidronic acid anodizing at the appropriate anodizing voltage and electrolyte temperature. The highest self-ordering anodizing voltage achieved without burning exceeded 280 V by the stepwise voltage increase method. Selective dissolution of the anodic porous alumina caused the formation of a highly ordered submicrometer-scale dimple array on the aluminum substrate. The aluminum surface led to bright structural color with a rainbow spectrum due to the submicrometer-scale, periodic nanostructure of the substrate and reflected light mostly in the visible region, 490-760 nm. These highly ordered nanostructures of aluminum and its oxide can be used in various nanotechnology applications, such as in large-scale nanotemplates, nanofilters, and optical devices.

Acknowledgments

This research was conducted at Hokkaido University and was supported by the "Nanotechnology Platform" Program of the Ministry of Education, Culture, Sports, Science, and Technology (MEXT), Japan. The work was financially supported by the Japan Society for the Promotion of Science (JSPS) "KAKENHI" and Toyota Physical & Chemical Research Institute Scholars.

References

1) J.P. O'Sullivan, G.C. Wood, The morphology and mechanism of formation of porous anodic films on aluminium, Proceedings of the Royal Society A 317 (1970) 511.
2) G.E. Thompson, G.C. Wood, Porous anodic film formation on aluminium, Nature 290 (1981) 230.
3) G.E. Thompson, Porous anodic alumina: fabrication, characterization and applications, Thin Solid Films 297 (1997) 192.
4) H. Masuda, K. Fukuda, Ordered metal nanohole arrays made by a two-step replication of honeycomb structures of anodic alumina, Science 268 (1995) 1466.
5) W. Lee, S.-J. Park, Porous anodic aluminum oxide: anodization and templated synthesis of functional nanostructures, Chemical Reviews 114 (2014) 7487.
6) I. Turkevych, V. Ryukhtin, V, Garamus, S. Kato, T. Takamasu, G. Kido, M. Kondo, Studies of self-organization processes in nanoporous alumina membranes by small-angle neutron scattering, Nanotechnology 23 (2012) 325606.
7) C. Cheng, K.Y. Ng, N.R. Aluru, A.H.W. Ngan, Simulation and experiment of substrate aluminum grain orientation dependent self-ordering in anodic porous alumina, Journal of Applied Physics 113 (2013) 204903.
8) J.E. Houser, K.R. Hebert, The role of viscous flow of oxide in the growth of self-ordered porous anodic alumina films, Nature Materials 8 (2009) 415.
9) K.R. Hebert, S.P. Albu, I. Paramasivam, P. Schmuki, Morphological instability leading to formation of porous anodic oxide films, Nature Materials 11 (2012) 162.

10) H. Masuda, F. Hasegwa, S. Ono, Self-ordering of cell arrangement of anodic porous alumina formed in sulfuric acid anodizing, Journal of the Electrochemical Society 144 (1997) L127.
11) A.P. Li, F. Müller, A. Birner, K. Nielsch, U. Gösele, Hexagonal pore arrays with a 50–420 nm interpore distance formed by self-organization in anodic alumina, Journal of Applied Physics, 84 (1998) 6023.
12) O. Jessensky, F. Müller, U. Gösele, Self-organized formation of hexagonal pore arrays in anodic alumina, Applied Physics Letters 72 (1998) 1173.
13) O. Nishinaga, T. Kikuchi, S. Natsui, R.O. Suzuki, Rapid fabrication of self-ordered porous alumina with 10-/sub-10-nm-scale nanostructures by selenic acid anodizing, Scientific reports 3 (2013) 2748.
14) T. Kikuchi, O. Nishinaga, S. Natsui, R.O. Suzuki, Self-ordering behavior of anodic porous alumina via selenic acid anodizing, Electrochimica Acta 137 (2014) 728.
15) S. Ono, M. Saito, H. Asoh, Self-ordering of anodic porous alumina formed in organic acid electrolytes, Electrochimica Acta 51 (2005) 827.
16) H. Masuda, K. Yada, A. Osaka, Self-ordering of cell configuration of anodic porous alumina with large-size pores in phosphoric acid solution, Japanese Journal of Applied Physics 37 (1998) L1340.
17) K. Nielsch, J. Choi, K. Schwirn, R.B. Wehrspohn, U. Gösele, Self-ordering regimes of porous alumina: The 10% porosity rule, Nano Letters 2 (2002) 677.
18) W. Lee, R. Ji, U. Gösele, K. Nielsch, Fast fabrication of long-range ordered porous alumina membranes by hard anodization, Nature Materials 5 (2006) 741.
19) W. Lee, K. Schwirn, M. Steinhart, E. Pippel, R. Schols, U. Gösele, Structural engineering of nanoporous anodic aluminium oxide by pulse anodization of aluminium, Nature Nanotechnology 3 (2008) 234.
20) K. Schwirn, W. Lee, R. Hillebrand, M. Steinhart, K. Nielsch, U. Gösele, Self-ordered anodic aluminum oxide formed by H_2SO_4 hard anodization, ACS Nano 2 (2008) 302.
21) B. Sun, J. Li, X. Jin, C. Zhou, Q. Hao, X. Gao, Self-ordered hard anodization in malonic acid and its application in tailoring alumina taper-nanopores with continuously tunable periods in the range of 290-490 nm, Electrochimica Acta 112 (2013) 327.
22) W.J. Stępniowski, M. Norek, M. Michalska-Domańska, D. Forbot, A. Król, Study on the correlation between criterion number derived from Rayleigh–Bénard convective cells and arrangement of nanoporous anodic aluminum oxide, Materials Letters 125 (2014) 124.
23) M.A. Kashi, A. Ramazani, M. Rahmandoust, M. Noormohammadi, The effect of pH and composition of sulfuric–oxalic acid mixture on the self-ordering configuration of high porosity alumina nanohole arrays, Journal of Physics D: Applied Physics 40 (2007) 4625.
24) M.A. Kashi, A. Ramazani, M. Noormohammadi, M. Zarei, P. Marashi, Optimum

self-ordered nanopore arrays with 130–270 nm interpore distances formed by hard anodization in sulfuric/oxalic acid mixtures, Journal of Physics D: Applied Physics 40 (2007) 7032.
25) T. Kondo, H. Miyazaki, K. Nishio, H. Masuda, Surface-enhanced raman scattering on multilayered nanodot arrays obtained using anodic porous alumina mask, Journal of Photochemistry and Photobiology A: Chemistry 221 (2011) 199.
26) G.L. Hornyak, C.J. Patrissi, S.R. Martin, Fabrication, characterication, and optical properties of gold nanoparticle/porous alumina composites: The nonscattering Maxwell-Garnett limit, The Journal of Physical Chemistry B 101 (1997) 1548.
27) T. Yanagishita, K. Nishio, H. Masuda, Anti-reflection structures on lenses by nanoimprinting using ordered anodic porous alumina, Applied Physics Express 2 (2009) 022001.
28) T. Yanagishita, M. Masui, N. Ikegawa, H. Masuda, Fabrication of polymer antireflection structures by injection molding using ordered anodic porous alumina mold, Journal of Vaccum Science & Technology B 32 (2014) 021809.
29) T. Yanagishita, K. Nishio, H. Masuda, Two-dimensional photonic crystal composed of ordered polymer nanopillar arrays with high aspect ratios using anodic porous alumina templates, Applied Physics Express 1 (2008) 012002.
30) J. Choi, Y. Luo, R.B. Wehrspohn, R. Hillebrand, J. Schilling, U. Gösele, Perfect two-dimensional porous alumina photonic crystals with duplex oxide layers, Journal of Applied Physics 94 (2003) 4757.
31) S. Zhang, L. Wang, C. Xu, D. Li, L. Chen, D. Yang, Fabrication of Ni-NiO-Cu metal-insulator-metal tunnel diodes via anodic aluminum oxide templates, ECS Solid State Letters 2 (2013) Q1.
32) X. Zhao, G. Meng, F. Han, X. Li, B. Chen, Q. Xu, X. Zhu, Z, Chu, M. Kong, Q. Huang, Nanocontainers made of various materials with tunable shape and size, Scientific Reports 3 (2013) 2238.
33) T. Yanagishita, Y. Tomabechi, K. Nishio, H. Masuda, Preparation of monodisperse SiO_2 nanoparticles by membrane emulsification using ideally ordered anodic porous alumina, Langmuir 20 (2004) 554.
34) T. Yanagishita, M. Kawamoto, N. Nishio, H. Masuda, Fabrication of monodisperse particles by nanoimprinting using anodic porous alumina molds, Journal of Vacuum Science & Technology B 32 (2014) 011802.
35) A. Mozalev, R. Calavia, R.M. Vázquez, I. Gràcia, C. Cané, X. Correig, X. Vilanova, F. Gispert-Guirado, J. Hubálek, E. Llobet, MEMS-microhotplate-based hydrogen gas sensor utilizing the nanostructured porous-anodic-alumina-supported WO_3 active layer, International Journal of Hydrogen Energy 38 (2013) 8011.
36) A. Mozalev, R. M. Vázquez, C. Bittencourt, D. Cossement, F. Gispert-Guirado, E. Llobet, H. Habazaki, Formation–structure–properties of niobium-oxide nanocolumn arrays via self-organized anodization of sputter-deposited aluminum-on-niobium layers, Journal of Materials Chemistry C 2 (2014) 4847.

37) M. Almasi-Kashi, A. Ramazani, F. Kheyri, E. Jafari-Khamse, The effect of magnetic layer thickness on magnetic properties of Fe/Cu multilayer nanowires, Materials Chemistry and Physics 144 (2014) 230.
38) T. Kikuchi, T. Yamamoto, and R.O. Suzuki, Growth Behavior of Anodic Porous Alumina Formed in Malic Acid Solution, Applied Surface Science, 284 (2013) 907.
39) S.Z. Chu, K. Wada, S. Inoue, M. Isogai, Y. Katsuta, A. Yasumori, Large-scale fabrication of ordered nanoporous alumina films with arbitrary pore intervals by critical-potential anodization, Journal of the Electrochemical Society 153 (2006) B384.
40) S. Ono, M. Saito, M. Ishiguro, H. Asoh, Controlling factor of self-ordering of anodic porous alumina, Journal of the Electrochemical Society 151 (2004) B473.
41) Y. Katsuta, A. Yasumori, K. Wada, K. Kurashia, S. Suehara, S. Inoue, Three-dimensionally nanostructured alumina film on glass substrate: anodization of glass surface, Journal of Non-Crystalline Solids 354 (2008) 451.
42) J. Bellemare, F. Sirois, D. Ménard, Fabrication of micrometer-scale self-organized pore arrays in anodic alumina, Journal of the Electrochemical Society 161 (2014) E75.
43) X. Chen, D. Yu, L. Gao, X. Zhu, Y. Song, H. Huang, L. Lu, X. Chen, Fabrication of ordered porous anodic alumina with ultra-large interpore distance using ultrahigh voltages, Materials Research Bulletin 57 (2014) 116.
44) S.-F. Leung, M. Yu, Q. Lin, K. Kwon, K.-L. Ching, L. Gu, K. Yu, Z. Fan, Efficient photon capturing with ordered three-dimensional nanowell arrays, Nano Letters 12 (2012) 3682.
45) A. Zahariev, I. Kanazirski, A. Girginov, Anodic alumina films formed in sulfamic acid solution, Inorganica Chimica Acta 361 (2008) 1789.
46) M. Pashchanka, J. Schneider, Experimental validation of the novel theory explaining self-organization in porous anodic alumina films, Physical Chemistry Chemical Physics 15 (2013) 7070.
47) T. Kikuchi, T. Yamamoto, S. Natsui, R.O. Suzuki, Fabrication of anodic porous alumina by squaric acid anodizing, Electrochimica Acta 123 (2014) 14.
48) T. Kikuchi, O. Nishinaga, S. Natsui, R.O. Suzuki, Fabrication of anodic porous alumina via acetylenedicarboxylic acid anodizing, ECS Electrochemistry Letters 3 (2014) C25.
49) T. Kikuchi, D. Nakajima, J. Kawashima, S. Natsui, R.O. Suzuki, Fabrication of anodic porous alumina via anodizing in cyclicoxocarbon acids, Applied Surface Science 313 (2014) 276.
50) K.D. Demadis, M. Paspalaki, J. Theodorou, Controlled release of bis (phosphonate) pharmaceuticals from cationic biodegradable polymeric matrices, Industrial & Engineering Chemistry Research 50 (2011) 5873.
51) K. Popov, H. Rönkkömäki, L.H. Lajunen, Critical evaluation of stability constants of phosphonic acids (IUPAC technical report), Pure and applied chemistry 73 (2001)

1641.

Captions

Fig. 1 a) Changes in anodizing voltage, U, with time, t, during anodizing in a 0.3 M etidronic acid solution at 293 K and different constant current densities of 10-30 Am^{-2}. b), c), d) SEM images of the surface, interface, and vertical cross-section of the specimen anodized at 30 Am^{-2} for 60 min.

Fig. 2 Changes in current density, j, with anodizing time, t, during anodizing in a 0.3 M etidronic acid solution at a) 293 and b) 273 K and constant cell voltages in the range of U = 250-295 V.

Fig. 3 Changes in current density, j, with anodizing time, t, during anodizing in a 0.3 M etidronic acid solution at a) 2983, b) 303, c) 313 K, and c) 333 K and constant cell voltages in the range of U = 145-245 V.

Fig. 4 Effects of temperature, T, on the highest anodizing voltage, U, for etidronic acid anodizing.

Fig. 5 SEM images of the submicrometer-scale dimple array formed on the aluminum substrate after etidronic acid anodizing at 313 K and different voltages of a) 190 V, b) 200 V, and c) 210 V for 120 min.

Fig. 6 SEM images the dimple array formed on the aluminum substrate after etidronic acid anodizing under the following anodizing conditions: a) at 225 V and 303 K for 480 min, b) at 240 V and 298 K for 480 min (8 h), and c) 270 V and 293 K for 960 min (16 h).

Fig. 7 SEM images of the dimple array formed on the aluminum substrate after etidronic acid anodizing at the same anodizing voltage of 270 V and a) 293 K for 120 min and b) 273 K for 4320 min (72 h).

Fig. 8 a) Changes in current density, j, with anodizing time, t, during etidronic acid anodizing (293 K) by directly applying a voltage of 275 V and by a) the stepwise voltage increase method at 270 V for 120 min, 275 V for 120 min, and 280 V for 120 min. b) SEM image of the dimple array formed on the aluminum substrate after anodizing by increasing the voltage in a stepwise manner.

Fig. 9 SEM images of the fracture cross-section of the highly ordered anodic porous alumina fabricated via two-step anodizing at 270 V.

Fig. 10 a) The relation between the self-ordering voltage, U_s, and the electrolyte temperature, T, during etidronic acid anodizing. b) The relation between the cell

diameter, D, and the self-ordering voltage, U_s, for anodic porous alumina formed in various acidic electrolytes (sulfuric, oxalic, selenic, malonic, phosphoric, and tartaric acid) reported previously, as well as that for the alumina specimen formed in etidronic acid observed in the present investigation.

Fig. 11 a) Bright structural colors obtained from the nanostructured aluminum specimen at different viewing angles. b) Reflection spectrum of the nanostructured aluminum specimen at different angles under white-light irradiation. c) A schematic illustration of the reflection measurements obtained from the nanostructured aluminum specimen.

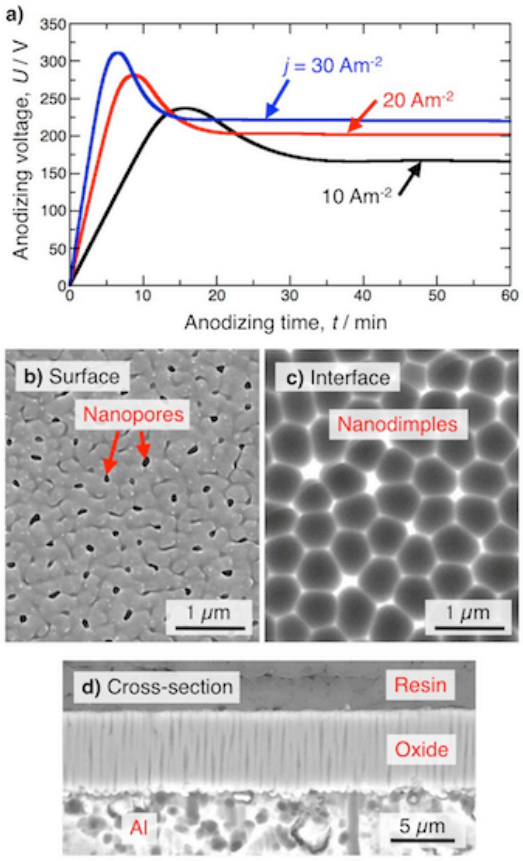
a)
Anodizing voltage, U / V
Anodizing time, t / min
j = 30 Am-2
20 Am-2
10 Am-2
b) Surface
Nanopores
1 μm
c) Interface
Nanodimples
1 μm
d) Cross-section
Resin
Oxide
Al
5 μm

Figure 1.

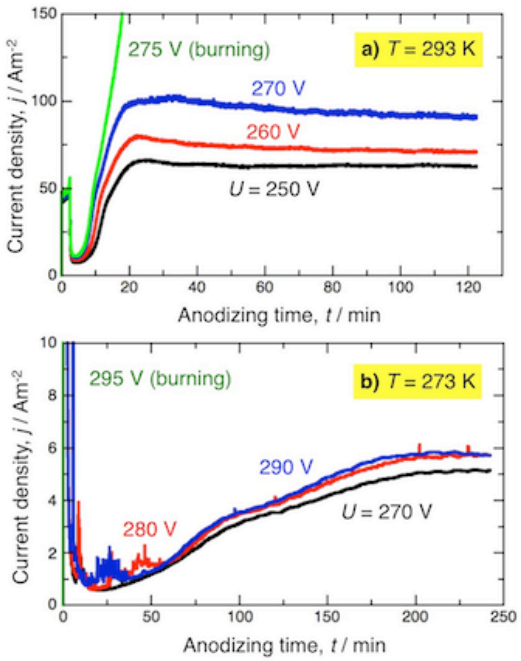
a) T = 293 K
275 V (burning)
270 V
260 V
U = 250 V
Current density, j / Am-2
Anodizing time, t / min
b) T = 273 K
295 V (burning)
290 V
280 V
U = 270 V
Current density, j / Am-2
Anodizing time, t / min

Figure 2.

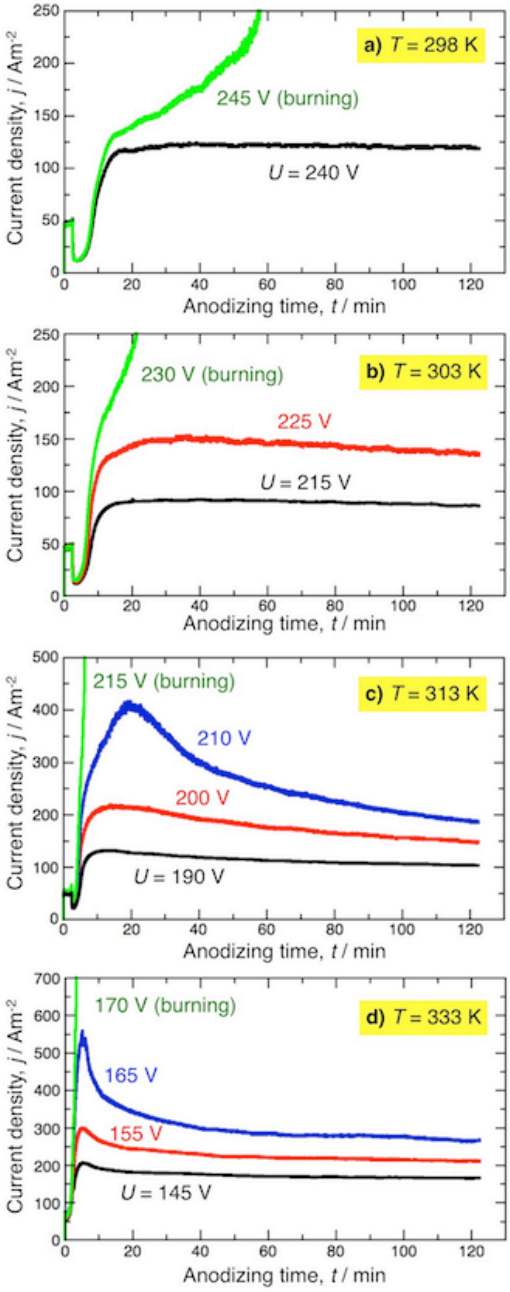
a) T = 298 K
245 V (burning)
U = 240 V
b) T = 303 K
230 V (burning)
225 V
U = 215 V
c) T = 313 K
215 V (burning)
210 V
200 V
U = 190 V
d) T = 333 K
170 V (burning)
165 V
155 V
U = 145 V
Current density, j / Am-2
Anodizing time, t / min

Figure 3.

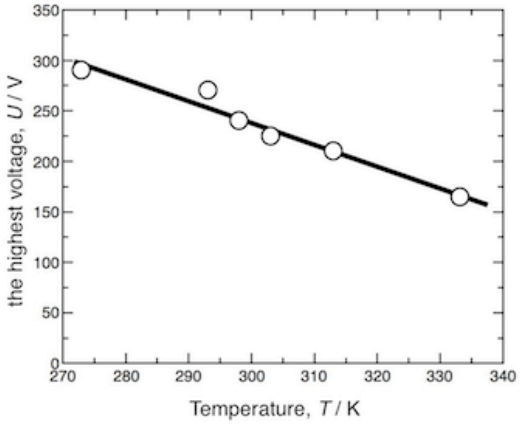
the highest voltage, U / V
Temperature, T / K
350
300
250
200
150
100
50
0
270
280
290
300
310
320
330
340

Figure 4.

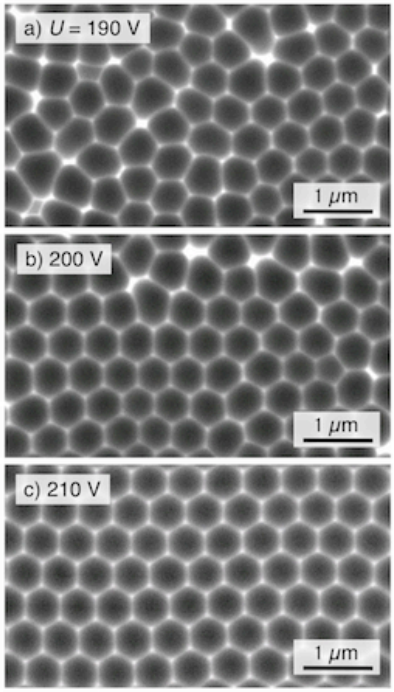

Figure 5.

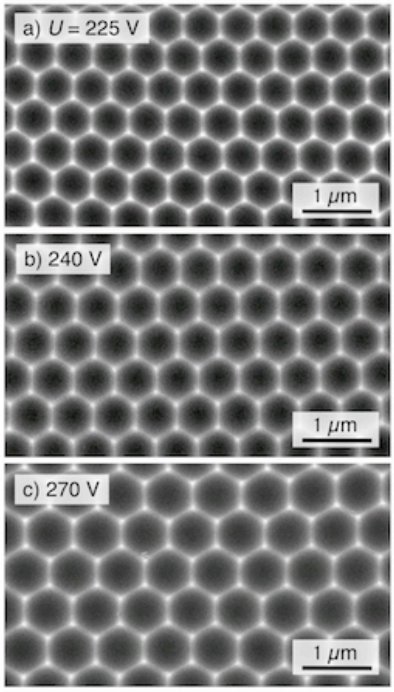

Figure 6.

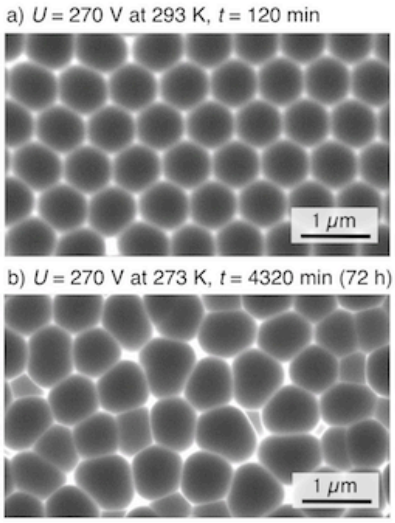

Figure 7.

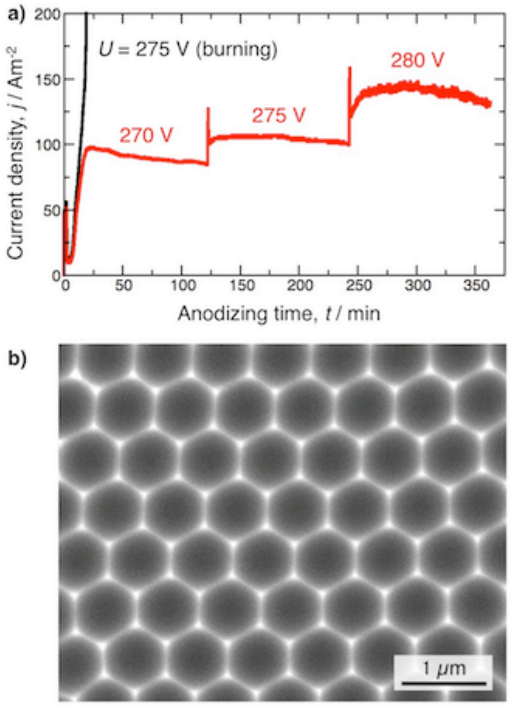
a)
200
150
100
50
0
Current density, j / Am-2
U = 275 V (burning)
270 V
275 V
280 V
0
50
100
150
200
250
300
350
Anodizing time, t / min
b)
1 μm

Figure 8.

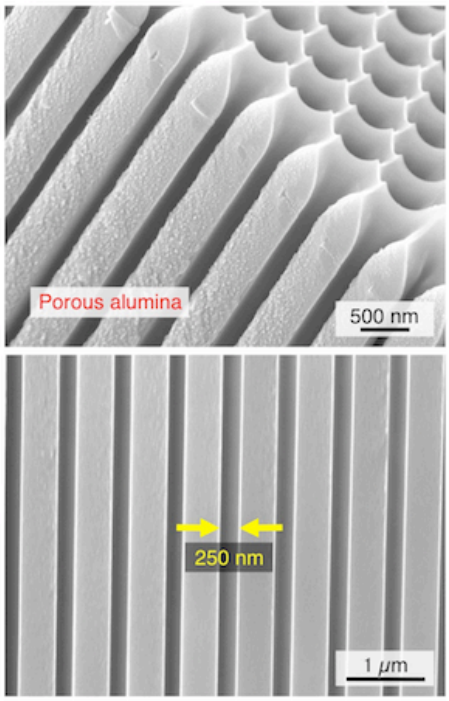

Figure 9.

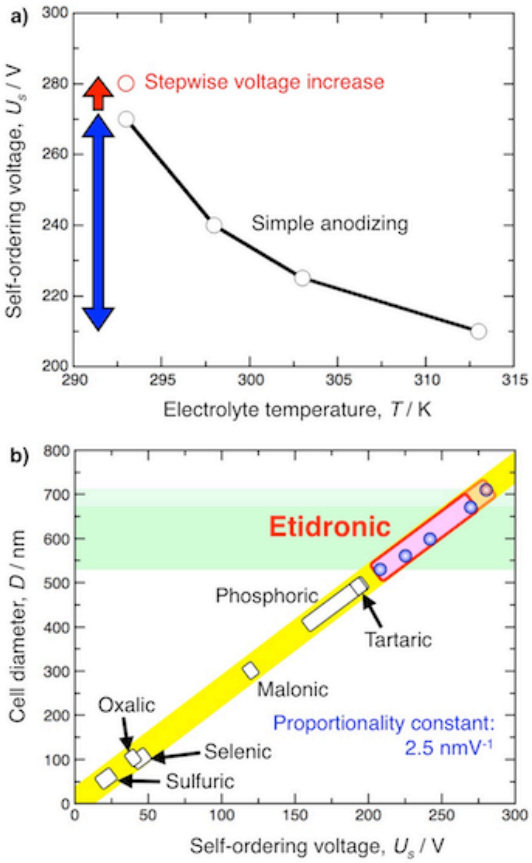
a)
Stepwise voltage increase
Simple anodizing
Self-ordering voltage, U_s / V
Electrolyte temperature, T / K
b)
Etidronic
Phosphoric
Tartaric
Malonic
Oxalic
Selenic
Sulfuric
Proportionality constant:
2.5 nmV^{-1}
Cell diameter, D / nm
Self-ordering voltage, U_s / V

Figure 10.

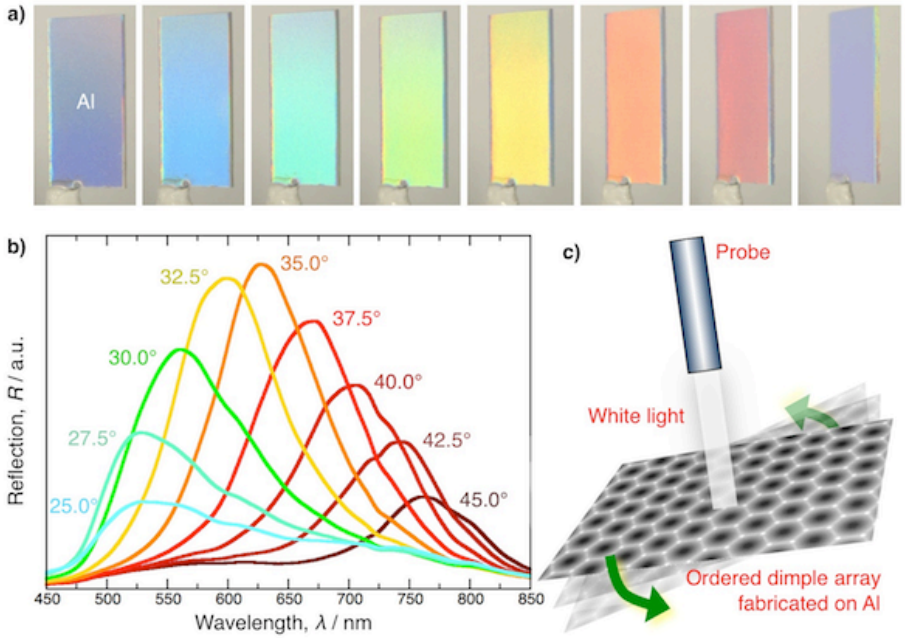
a)
Al
b)
Reflection, R / a.u.
Wavelength, λ / nm
450
500
550
600
650
700
750
800
850
25.0°
27.5°
30.0°
32.5°
35.0°
37.5°
40.0°
42.5°
45.0°
c)
Probe
White light
Ordered dimple array
fabricated on Al

Figure 11.